Right ventricular dysfunction in critically ill COVID-19 ARDS

Caroline Bleakley [a,b,1], Suveer Singh [b,1], Benjamin Garfield [b,1], Marco Morosin [b,1], Elena Surkova [d,1], Ms Sundhiya Mandalia [c,1], Bernardo Dias [d,1], Emmanouil Androulakis [a,1], Laura C. Price [e,1], Colm McCabe [e,1], Stephen John Wort [e,1], Cathy West [d,1], Wei Li [a,d,1], Rajdeep Khattar [a,d,1], Roxy Senior [a,d,1], Brijesh V. Patel [b,1], Susanna Price [a,b,*,1]

[a] Department of Cardiology, Royal Brompton Hospital, Sydney Street, London, UK
[b] Department of Adult Critical Care, Royal Brompton Hospital, Sydney Street, London, UK
[c] Department of Medical Statistics, Imperial College, London, UK
[d] Department of Echocardiography, Royal Brompton Hospital, Sydney Street, London, UK
[e] Pulmonary Hypertension Service, Royal Brompton Hospital, Sydney Street, London, UK

A R T I C L E   I N F O

A B S T R A C T

Aims: Comprehensive echocardiography assessment of right ventricular (RV) impairment has not been reported in critically ill patients with COVID-19. We detail the specific phenotype and clinical associations of RV impairment in COVID-19 acute respiratory distress syndrome (ARDS).
Methods: Transthoracic echocardiography (TTE) measures of RV function were collected in critically unwell patients for associations with clinical, ventilatory and laboratory data.
Results: Ninety patients (25.6% female), mean age 52.0 ± 10.8 years, veno-venous extracorporeal membrane oxygenation (VVECMO) (42.2%) were studied. A significantly higher proportion of patients were identified as having RV dysfunction by RV fractional area change (FAC) (72.0%,95% confidence interval (CI) 61.0–81.0) and RV velocity time integral (VTI) (86.4%, 95 CI 77.3–93.2) than by tricuspid annular plane systolic excursion (TAPSE) (23.8%, 95 CI 16.0–33.9), RVS' (11.9%, 95% CI 6.6–20.5) or RV free wall strain (FWS) (35.3%, 95% CI 23.6–49.0). RV VTI correlated strongly with RV FAC ($p \leq 0.01$). Multivariate regression demonstrated independent associations of RV FAC with NTpro-BNP and PVR. RV-PA coupling correlated with PVR (univariate $p < 0.01$), as well as RVEDAi ($p < 0.01$), and RVESAi ($p < 0.01$), and was associated with P/F ratio (p 0.026), PEEP (p 0.025), and ALT (p 0.028).
Conclusions: Severe COVID-19 ARDS is associated with a specific phenotype of RV radial impairment with sparing of longitudinal function. Clinicians should avoid interpretation of RV health purely on long-axis parameters in these patients. RV-PA coupling potentially provides important additional information above standard measures of RV performance in this cohort.

1. Introduction

The coronavirus disease 2019 (COVID-19) caused by severe acute respiratory syndrome coronavirus 2 (SARS-CoV-2) [1] has reached pandemic levels. At the time of writing there have been over 50 million cases confirmed and 1.2 million deaths worldwide [2]. Whilst the majority of patients with COVID-19 have suffered a relatively mild course, there has been an unprecedented burden on critical care from the 5% of patients who develop critical illness [3]. COVID-19 is a complex and evolving multi-organ disease with cardiovascular effects that will not be fully understood while the pandemic is ongoing. The true cardiovascular impact of this will not be fully understood until longer-term follow-up data becomes available, particularly with respect to the coronary ischaemic burden and prevalence of heart failure. While the pandemic is ongoing, efforts are therefore focused on identifying acute cardiac complications, more common in those with severe disease and associated with increased mortality [4,5]. To date, reported cardiovascular consequences of COVID-19 include ST elevation myocardial infarction [6], myocarditis, heart failure, pulmonary embolism (PE), arrhythmia, sudden death, and pulmonary hypertension [7]. Reconfiguration of non-invasive diagnostic cardiology services during the pandemic has placed emphasis on bedside transthoracic echocardiography (TTE), as recommended by the European and American Societies [7,8].

Currently, limited information is available on the impact of COVID-19 on the right heart, particularly in a critical care cohort [9]. Tricuspid annular plane systolic excursion (TAPSE), a standard measure of right ventricular (RV) function, has been reported to be abnormal in only 4% of unselected hospitalised patients with COVID-19 [10]. The largest TTE study to date has identified RV free wall strain (RVFWS) as a better predictor of mortality in patients with COVID-19 than either TAPSE or RV systolic velocity (RVS'). This suggests the need to examine potentially important alternative measures of RV dysfunction in this cohort [11]. We therefore examined TTE, clinical and laboratory data from patients admitted to our cardiothoracic critical care units to establish the pattern, clinical determinants and burden of RV dysfunction in severe COVID-19 ARDS.

2. Methods

2.1. Study design

This was an observational study of retrospectively collected data on laboratory confirmed SARS-CoV-2 patients who were invasively ventilated at the Royal Brompton Hospital, London, UK between 20th March – 22nd April 2020. The study was registered locally and was conducted as a service evaluation as defined by the U.K. NHS Health Research Authority (http://www.hra.nhs.uk) using anonymous, routinely collected data and therefore did not require review by the Research Ethics Committee.

2.2. Outcome measures

The primary outcome measure was the proportion of patients identified as having RV dysfunction by different measures: tricuspid annular plane systolic excursion (TAPSE); RV systolic velocity (RVS'); RV fractional area change (RV FAC); RV velocity time integral (RV VTI). The associations between echocardiographic measures of RV dysfunction and size, pulmonary vascular measures, clinical, laboratory and ventilatory parameters were analysed. RV-pulmonary artery (PA) coupling, using the FAC:RV systolic pressure (RVSP) ratio was analysed to determine its added value against other measures of RV dysfunction.

2.3. Clinical, laboratory and ventilation data

Baseline characteristics, co-morbidity, clinical and laboratory data were captured from critical care electronic patient records from the first 24 h after admission to ICU. Laboratory data included alanine aminotransferase (ALT), NT-pro-brain natriuretic peptide (BNP), C-reactive protein (CRP), D-dimer, estimated glomerular filtration rate (eGFR) and highly sensitive troponin I (hs-TnI). Ventilation parameters including positive end expiratory pressure (PEEP) and partial pressure of oxygen/inspired oxygen (PaO_2/FiO_2) ratio were recorded as an average value on the first day of admission. The severity of ARDS was numerically categorized as a Murray Score [12].

2.4. Transthoracic echocardiography

All studies were performed using Philips CVX ultrasound (Philips Medical Systems, Andover, MA, USA) in accordance with published recommendations [13] within the first 24 h of admission to ICU. Analysis of 2D imaging was performed offline by an experienced cardiologist blinded to the clinical data. i) Measures of RV performance (TAPSE, RVS', RV FAC and RV VTI) and size (RV end diastolic area (EDA) and RV end systolic area (ESA)) were performed in accordance with the published recommendations and indexed to BSA. Maximal TAPSE was obtained with M-mode through the lateral tricuspid annulus. ii) Doppler indicators were acquired over averaged consecutive beats using sweep speeds of 100 cm/s. iii) Estimates of pulmonary pressure were calculated from the peak gradient of tricuspid regurgitation using the

modified Bernoulli formula added to the central venous pressure. Pulmonary vascular resistance (PVR) was calculated according to the published formula [14]. iv) RV-PA coupling was estimated using a parameter of RV function against pulmonary pressure as estimated by RVSP (FAC/RVSP was used to define this measure). v) Left ventricular (LV) 2D ejection fraction was calculated using the published Simpson's biplane method of discs [13]. Filling pressure was estimated using the published mitral inflow and tissue Doppler methods (E/e' averaged from the septal and lateral annulus readings) [15]. Tissue Doppler imaging (TDI) of the mitral and tricuspid annulus measured maximal systolic excursion velocity (S', in cm/s), and maximal diastolic velocity (e') using a pulsed tissue Doppler 5 mm sample volume placed at the lateral tricuspid annulus, and lateral and septal mitral annulus in the apical four-chamber view, with a high-pass filter to eliminate high-velocity interference [15].

2.5. RV strain analysis

RV strain analysis was performed on the commercially available TomTec platform (TomTec Imaging Systems, Germany) using one selected cardiac cycle from the apical focussed RV view with an adequate frame rate (≥60 frames/s) as per the published guidance [5]. Having identified the required landmarks in the systolic frame, the generated region of interest can then be manually edited as required. The software recognises and divides the RV free wall and septum into 3 segments respectively; basal, mid and apical. RV strain was defined as the end-systolic negative value of the longitudinal strain curve for RV free wall strain (RVFWS). RV strain was calculated only if tracking was adequate in at least five segments.

2.6. Statistical analysis

Quantitative data that are normally distributed are presented as mean with standard deviation while non-normally distributed data are presented as median with inter-quartile range. Categorical data are presented as frequency and percentages (%) and compared using the χ^2 test and where numbers in cells were low, Yate's correction was applied. Between group comparison of normally distributed data were tested using unpaired t-test while between group comparisons of non-normally distributed data were assessed using the Mann-Whitney U test. Pearson's correlation coefficient was derived on quantitative data which were either normally distributed or after variance stabilising transformation was applied. Univariate linear regression analysis was used to assess associations between quantitative variables and where applicable, variance stabilising transformation using log10 was used. Those variables that were found to be significant at p < 0.15 in univariate linear regression model were used to derive a multivariable linear regression model. All statistical analyses were performed using SAS version 9.4 and GraphPad Prism version 8, all p-values presented are two tailed.

3. Results

We studied 90 consecutive mechanically ventilated patients (42.2% VV-ECMO) admitted to the adult intensive care units at the Royal Brompton Hospital, London, UK. The demographic and clinical characteristics of the cohort are described in Table 1. Table 2 outlines the demographic echocardiography data as well as the number of patients in whom echocardiography was possible. In summary, the mean age of the cohort was 52.0 ± 10.8 years (25.6% female) with the most prevalent comorbidities being hypertension and diabetes mellitus (36.7% and 22.2%, respectively) and 22.3% on treatment with an angiotensin converting enzyme inhibitor or angiotensin receptor blocker.

Table 1

Demographics of 90 consecutive patients diagnosed with COVID-19 on the Intensive Care Unit at the Royal Brompton Hospital who underwent echocardiography. Ethnicity (1 = Caucasian, 2 = Asian, 3 = black). Body surface area (BSA), Body mass index (BMI), Hypertension (HTN), Diabetes (DM), Chronic obstructive pulmonary disease (COPD), chronic kidney disease (CKD), Angiotensin converting enzyme inhibitor (ACEi) angiotensin receptor blocker (ARB), Brain natriuretic peptide (BNP), Positive end expiratory pressure (PEEP), Alanine aminotransferase (ALT), high sensitivity C-reactive protein (hsCRP), (hs-TnI) high-sensitivity troponin I, (eGFR) estimated glomerular filtration rate.

		Mean (sd) /Median (IQR) / n (%)	Total n
Age		52.0 (10.8)	90
Sex	Male	67 (74.4)	90
Ethnicity	1	38 (42.2)	88
	2	42 (46.7)	
	3	8 (8.9)	
BSA, m2		2.0 (0.2)	86
BMI, kg/m2		29. 5 (6.6)	85
VVECMO (n)		38 (42.2%)	90
Medical history			
HTN		33 (36.7%)	87
DM		20 (22.2%)	87
COPD		1 (1.1%)	87
CKD		2 (2.2%)	87
ACEi/ARB use		21 (23.3%)	84
Drug therapy			
Steroids		44 (48.9%)	87
Inotropes		19 (21.1%)	87
Vasopressors		84 (93.3%)	87
Ventilatory			
PaO$_2$:FiO$_2$ ratio		22.3 (10.1)	87
PEEP		11.2 (2.5)	85
Murray Score		3(2.8–3.3)	87
Laboratory measures			
ALT		45 (29–61)	87
D-dimer		3285(2162–8663)	84
hsCRP		266.8 (114.2)	87
Highest BNP		100 (52–226)	78
hs-TnI		169.6 (630.8)	86
eGFR		92.7 (68.6)	86

Table 2

Mean and standard deviation of measures of right heart function in critically unwell patients with COVID-19 who underwent echocardiography along with normal values and total number of patients having each measurement taken. Right ventricle fractional area change (RV FAC), Right ventricle velocity time integral (RV VTI), Tricuspid annular plane systolic excursion (TAPSE), Right ventricular S velocity (RVS'), Right ventricle free wall strain (RVFWS).

	Normal value	Mean(sd)	Total n
LVEF(%)	≥52 female	59.91(10.98)	80
LVOT VTI (cm)	>18	20.2 (5.2)	83
E/e'	<14	8.9 (2.2)	83
RVEDA (cm^2)	10–24	22.6(5.5)	76
RVEDAi (cm^2/m^2)	5–12.6	11.3(2.6)	76
RVESA (cm^2)	3–15	16.3(5.5)	76
RVESAi (cm^2/m^2)	2–7.4	8.2(2.6)	76
RV FAC, %	≥ 35	28.9(10.6)	75
RV VTI, cm	≥ 19	14.3(4.2)	81
TAPSE, mm	≥ 17	20.0(4.8)	84
RVS' (cm/s)	≥ 9.5	13.5(3.8)	84
RV free wall strain (%)	≥ −22	−24.1(6.9)	51
RVSP (mmHg)	<25	46.8(14.9)	65
PVR (WU)	<1.6	2.3(0.9)	65

3.1. Pattern of RV impairment in COVID-19 ARDS

Mean RV systolic function defined by RV FAC (28.9 ± 10.6%) and RV VTI (14.3 ± 4.2%) was reduced, while TAPSE (20 ± 4.8 mm), RVS' (13.5 ± 3.8 cm/s) and RVFWS (−24.1 ± 6.9%) were preserved (Table 2). A significantly higher proportion of patients were identified as having RV dysfunction by RV FAC and RV VTI than by TAPSE, RVS' and RVFWS (Fig. 1).
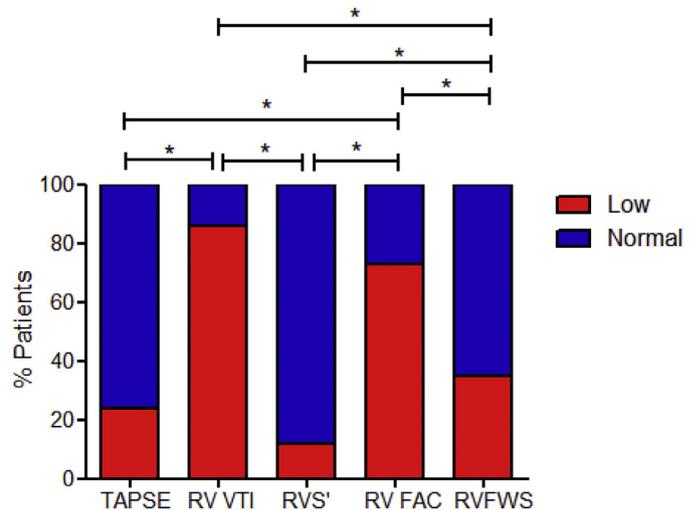
Fig. 1. Proportion of patients with COVID-19 admitted to critical care identified as having abnormal right ventricular function defined by different measures. The tricuspid annular plane systolic excursion (TAPSE) defined 23.8 (95 CI 16.0–33.9) % as having RV dysfunction and 76.2 (95% CI 66.1–84.0) % as having normal RV function. Right ventricular velocity time integral (RV VTI) defined 86.4 (95 CI 77.3–93.2) % as having RV dysfunction and 13.6 (95% CI 7.8–22.7)% as having normal RV function. Right ventricular systolic velocity (RVS') defined 11.9 (95% CI 6.6–20.5) % as having RV dysfunction and 88.1 (95% CI 79.4–93.4)% as having normal RV function. Right ventricular fractional area change (RV FAC) defined 72.0 (95% CI 61.0–81.0) % as having RV dysfunction and 28.0 (95% CI 19.0–39.0)% as having normal RV function. Right ventricular free wall strain (RVFWS) defined 35.3 (95% CI 23.6–49.0) % as having RV dysfunction and 64.7 (95% CI 51.0–76.4) % as having normal RV function. Chi squared 164.7, df 4, p < 0.001.

RV FAC and RV VTI were both associated with RV size by RVEDAi and RVESAi (Fig. 2A–D). Conversely, RVS' showed no correlation with RV size by RVEDAi on univariate regression (p 0.24) or with RVESAi (p 0.11), while TAPSE only correlated with RVESAi (Fig. 2E) (p 0.33).

RV VTI correlated strongly with reduction in RV FAC, whilst RVS' did not. TAPSE correlated with reduced RV FAC but this was numerically less significant (Fig. 3 A–C). In a subgroup (n = 51), an association was demonstrated on univariate regression between RVFWS and RV FAC (slope − 0.28 intercept −16.3 p 0.0023) and RVESAI (slope 0.86 intercept −31.48 p 0.016), but not with RVEDAi (p 0.14). There was no association between RVFWS and RVSP or PVR (univariate regression p 0.81; p 0.22, respectively). Further, there was no significant relationship between RVFWS and hs-TnI or NTpro-BNP levels (p 0.33; p 0.27, respectively).

3.2. Correlations of RV impairment measured by RV FAC

RV FAC correlated significantly with BNP, highly sensitive troponin I (hs-TnI) and echocardiographic measured pulmonary vascular resistance (PVR). RV FAC failed to correlate with RVSP, ventilation (defined by PEEP and P/F ratio), coagulopathy (defined by d-dimer), inflammation measured by CRP, liver function measured by ALT (Table 3). Intra-observer variability in RV FAC measurement over 10 separate studies was low with a mean difference of 0.29 (95% CI 0.65–1.23, p = 0.504).

3.3. RV-PA coupling

In addition to standard parameters we analysed echocardiographic derivations of RV-PA coupling to assess RV function in combination with its afterload. Falling ratios are broadly representative of uncoupling of the RV's ability to contract against its hydraulic load and have previously been linked with mortality outcomes [16]. RV FAC/RVSP was used in preference to other measures and had a mean value of 0.7 ± 0.3. Using a standard cut off for normal function of 1.0 this measure identified 85.9 (95% confidence interval (CI), 75.4–92.4)% of patients as having RV-PA uncoupling (n = 64). Previous work has
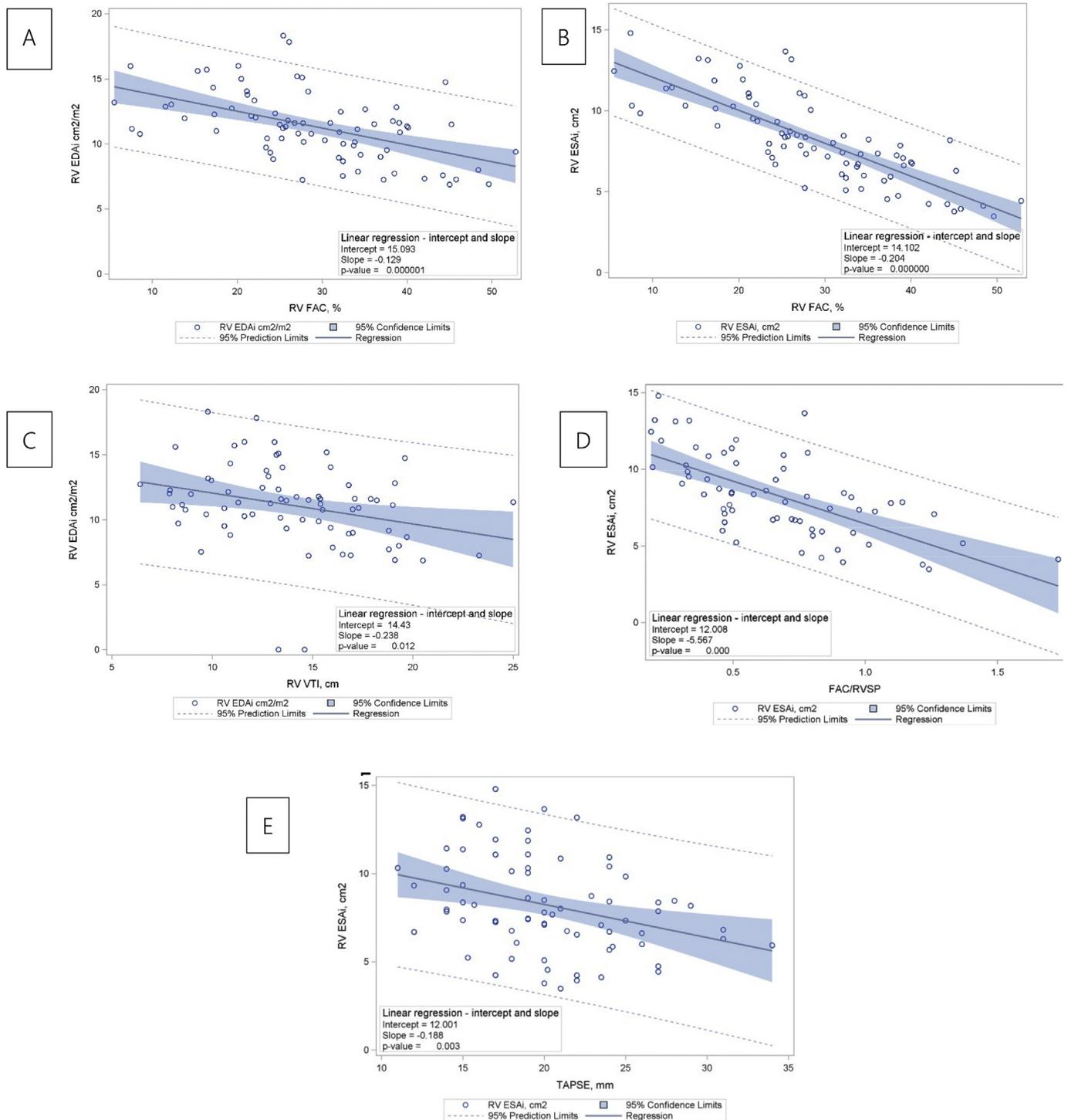
Fig. 2. Significant correlations of measures of right ventricular function and right ventricular size in critically unwell patients with COVID-19. A) Right ventricular fractional area change (RV FAC) is plotted against right ventricular end diastolic area index (REVDAI) and B) against indexed right ventricular end systolic area (RVESAi). C) Right ventricular velocity time integral (RV VTI) is plotted against RVEDAi and D) against RVESAi. E) Tricuspid annular plane systolic excursion (TAPSE) is plotted against RVESAi.

identified a RV FAC/RVSP of ≤0.6 as defining those with severe RV-PA uncoupling [17]. Using this cut off RV FAC/RVSP identified 46.9 (95% CI, 38.2–58.9)% of patients with COVID-19 on our intensive care unit as having significant RV-PA uncoupling. FAC/RVSP correlated significantly with PVR as well as RVEDAi and RVESAi (Fig. 4). RV FAC/RVSP was also associated with P/F ratio, PEEP, and ALT, with borderline association with NTpro-BNP (Table 4). It did not correlate with hs-TnI, D-dimer and CRP.

4. Discussion

The primary findings of this study are 1) there is a high burden of RV dysfunction in critically ill patients with COVID-19; 2) reliance on longitudinal parameters may miss the degree of impairment; 3) RV FAC correlates with markers of cardiac stress (hs-TnI and NTpro-BNP) and PVR; 4) RV-PA coupling is an important and previously unreported echocardiographic marker of severity in this cohort.
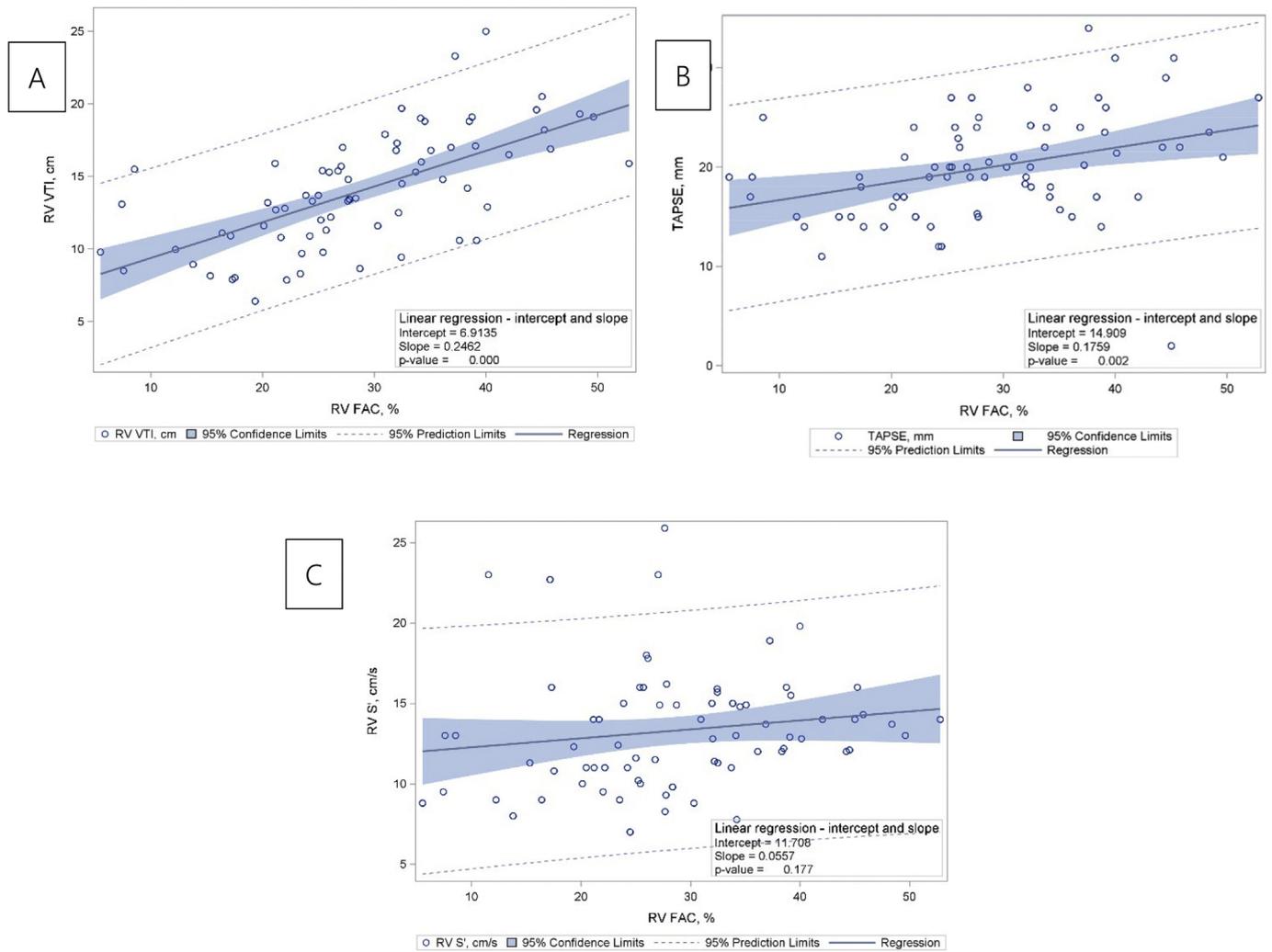
Fig. 3. Significant correlations between right ventricular fractional area change (RV FAC) and other measures of right ventricular function in critically unwell COVID-19 patients. A) RV FAC plotted against right ventricular velocity time integral (RV VTI). B) RV FAC plotted against tricuspid annular plane systolic excursion (TAPSE). C) RV FAC plotted against right ventricular S velocity (RVS').

Table 3

Univariate regression of right ventricular fractional area change (RV FAC) against baseline biochemical, ventilatory, inflammatory markers as well as echocardiographic measures of pulmonary hypertension in critically unwell patients with COVID-19. Brain natriuretic peptide (BNP), right ventricular systolic pressure (RVSP), pulmonary vascular resistance (PVR), positive end expiratory pressure (PEEP), alanine aminotransfersase (ALT), high sensitivity C-reactive protein (CRP).

Correlations with RV FAC	Gradient (intercept)	p-value
NTpro-BNP	−0.01 (29.6)	0.009
RVSP	−0.03 (29.9)	0.726
PVR	−5.2 (41.0)	<0.001
PaO$_2$:FiO$_2$ ratio	0.2 (25.5)	0.222
PEEP	−0.04 (29.7)	0.928
ALT	−0.05 (31.8)	0.098
D-dimer	−0.00004 (29.1)	0.769
hsCRP	0.02 (24.7)	0.162
TnI	−3.68 (34.34)	0.039

4.1. Phenotype of RV dysfunction in critical covid-19

ARDS is the predominant dictator of those admitted to critical care with COVID-19. The frequency and pattern of RV dysfunction in our cohort is quite different from that reported in non-COVID ARDS [18–20] and is emerging as an important feature of severe COVID-19 associated mortality [21]. Our data clearly demonstrates RV radial dysfunction rather than longitudinal impairment as the dominant phenotype. Measurement of long-axis function by TAPSE and RVS' therefore failed to identify the significant burden of RV impairment. In fact, in many cases these parameters were hyperdynamic in what may represent a compensatory response to radial dysfunction.

4.2. Comparison with non-covid-19 ARDS and non-critical covid-19 cohorts

Our data portrays a different picture of RV dysfunction from both non-COVID-19 ARDS and non-critical COVID-19 [22–24]. A recent large observational study reports important differences from our findings in a predominantly non-critical cohort [25]. RV abnormalities were reported in 185 of the 1216 patients studied, and was more common in more severe forms of COVID-19. In contrast to our data, there was no association between biomarker elevation (either troponin or natriuretic peptides) and incidence of RV dysfunction. The study did not report specific patterns of RV impairment and did not specify which parameters were used to determine RV function. However, previous data from single center studies of non-critical COVID-19 cohorts, consistently report a reduction in RV longitudinal rather than radial function [22,23,26].
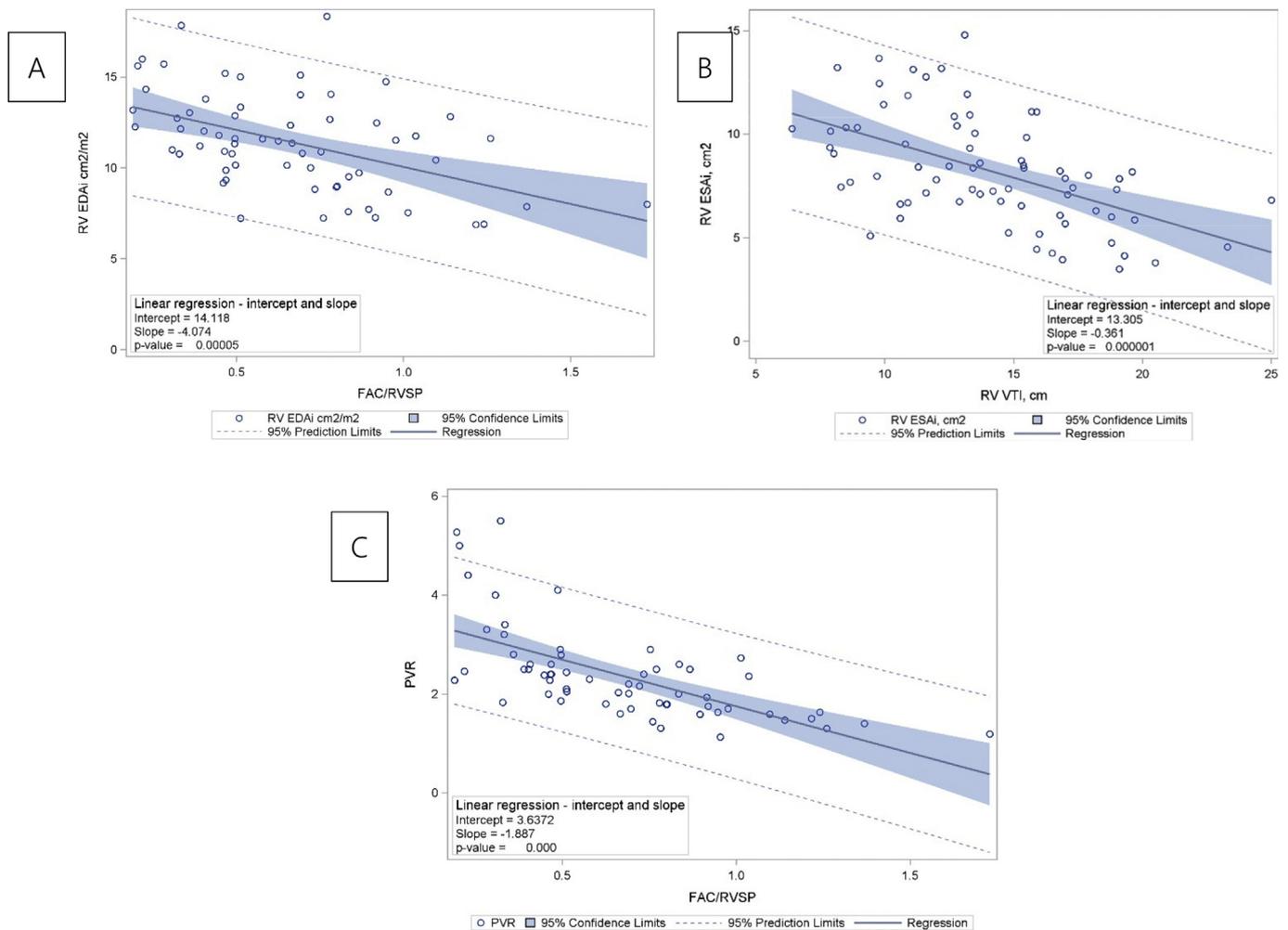
Fig. 4. Significant correlations of right ventricular size and pulmonary vascular resistance with right ventricular-pulmonary artery coupling measured by right ventricular fractional area change (RV FAC) / Right ventricular systolic pressure (RVSP) in critically unwell patients with COVID-19. A) RV FAC/RVSP plotted against indexed right ventricular end diastolic area (RVEDAi). B) RV FAC/RVSP plotted against indexed right ventricular end systolic area (RVESAi). C) RV FAC/RVSP plotted against pulmonary vascular resistance (PVR).

Table 4

Univariate regression of right ventricular fractional area change (RV FAC) / right ventricular systolic pressure (RVSP) against baseline biochemical, ventilatory, inflammatory markers in critically unwell patients with COVID-19. NTpro-Brain naturiretic peptide (BNP), positive end expiratory pressure (PEEP), Alanine aminotransfersase (ALT), high sensitivity C-reactive protein (CRP).

Correlations with RV FAC / RVSP	Gradient (intercept)	p-value
NTpro-BNP	397.2 (−264.1)	0.056
PaO$_2$:FiO$_2$ ratio	15.41 (8.99)	0.026
PEEP	12.27 (−2.03)	0.025
ALT	74.01 (−32.83)	0.028
D-dimer	9448 (−2876)	0.49
hsCRP	248.5 (40.96)	0.35
TnI	128.7 (135)	0.64

Comparing our data to non-COVID-19 ARDS cohorts, the pattern of isolated radial impairment has not been described. Briefly, the RV is of a different architecture to the LV, designed to deliver equivalent stroke volume to the lungs under lower pressure to avoid overwhelming the low resistance pulmonary capillary bed [18]. Its complex 3D geometry makes 2D assessment prone to regional variations, and there is precedent for the use of RV FAC over TAPSE as it has demonstrated superior correlation with 3D EF [27]. Data on RV performance in ARDS is rather limited and available studies have not universally examined the same echocardiography definitions; many reported septal dyskinesia and RVEDA/LVEDA ratio [18–20] rather than TAPSE or FAC. In the specific COVID-19 ARDS cohort that we studied, so far the largest relevant study of the RV that had a subset of ventilated ICU patients (N = 31) [28] did not specifically describe RV dysfunction but rather RV dilatation. RV enlargement is not uncommon during mechanical ventilation and there is no non-COVID ICU control group in the referenced study for comparison. Therefore, the degree of RV impairment that has emerged from our data is beyond that reported in both non-critical COVID-19 and previous ARDS cohorts, and the specific phenotype that we have identified is important in alerting clinicians of the need to avoid interpretation of RV health purely on long-axis parameters.

4.3. Potential mechanisms of RV dysfunction in critical covid-19

4.3.1. Intrinsic cardiac aetiology

The deterioration in RV radial function correlated strongly with hs-TnI and NTpro-BNP, indicators of cardiomyocyte injury and myocardial distension, respectively. This suggests either an intrinsic RV pathology, or that the RV is under stress from elevated afterload. Intrinsic RV dysfunction is conceivable given the reported incidence of myocarditis and ischaemic events in COVID-19 [4,5]. However, it is less likely given the relative sparing of the LV which would be assumed subject to the same insult in myocarditis. Ischaemia is another possible explanation, and the higher PVR and RVSP may be relevant here. Raised RV end

diastolic pressure is a substrate for sub-endocardial ischaemia as a pressure overloaded RV with raised intramural pressure and coronary sinus congestion is vulnerable to loss of coronary perfusion [29] [30]. The strong correlation between RV size and degree of dysfunction would seem to support an argument for the rise in hs-TnI and NT-pro BNP as markers of stretch rather than ischaemia. Interestingly, there are other potential mechanistic differences between the RV dysfunction we report in critical care and that found in non-critical cohorts. Markers of inflammation such as interleukin-6 (IL-6) have been shown to be linked with loss of longitudinal function in non-critical cohorts [22]. While we did not have access to IL-6 values, CRP did not correlate with RV dysfunction in our cohort, suggesting that loss of longitudinal function may be more susceptible to inflammatory or septic insult than radial.

4.4. Pulmonary afterload and loss of RV radial function

The strong correlation between RV impairment and elevated PVR further suggest that afterload was an important factor. There are distinct similarities between the phenotype of RV impairment demonstrated in our cohort and that seen in pulmonary hypertension (PH). Briefly, elevated pulmonary vascular tone in ARDS is a complex interplay of endothelial injury, hypoxic vasoconstriction, hypercapnia, acidaemia and pulmonary vascular remodelling [31,32]. The apparently selective loss of the subepicardial layer responsible for radial function in our study more resembles the pattern of myocardial remodelling seen in PH [33–35]. In PH, myocardial hypertrophy with disarray of fibre orientation and a significant change in 3-dimensional geometry creates an adapted RV with a disproportionate reduction in radial function [33–35]. The pattern is important as, should this resemble the PH model, there may be a substrate for disease regression and reverse remodelling [36]. The most plausible explanation based on the above correlations is a pooled aetiology of afterload and intrinsic RV pathology.

The effect of mechanical ventilation was also considered. Positive-pressure ventilation (PPV) can exacerbate lung stress by raising transpulmonary pressure, which is influenced by PEEP, tidal volume and lung compliance [37–39]. In our study, however, ventilator parameters had no significant impact on right heart function. This could be explained by the unusually high burden of pulmonary vascular micro-angiopathic pathology seen in severe COVID-19 pneumonia [40], reducing the relative impact of parenchymal disease and mechanical ventilation on PVR. Despite this, there was a lack of association between RV FAC and d-dimer. While coagulopathy is a recognised entity in the critically ill COVID-19 population [41], d-dimer is influenced by a wide range of factors including VVECMO [42]. The significant number of our patients on VVECMO, together with variable practice in anticoagulation and the arrival of patients at our hospital at differing points in their critical illness, may account for some of the variance and lack of association seen.

4.5. RV-PA coupling

In the present study, FAC:RVSP ratio correlated significantly not only with hs-TnI, NT-pro BNP and PVR but also with measures of ventilation (namely PEEP and PF ratio) and a liver marker of congestion (ALT). The RV is designed to remain coupled to its afterload with compensatory mechanisms inbuilt to withstand pressure changes in the circuit until these processes become overwhelmed and maladaptive [17]. The high compliance low resistance pulmonary circuit determines RV afterload and the RV is more adaptive to volume variation than pressure [30]. A preserved RV-PA coupling ratio reflects efficient coupling of RV effort to afterload, with a falling ratio signifying uncoupling of the RV's ability to face its hydraulic load [30,43]. In echocardiographic terms, more complex derivations of coupling have been simplified to relate measures of RV function to afterload and have been studied in heart failure [16]. Therefore, RV-PA coupling potentially offers additional

information on the causes and consequences of RV dysfunction in this cohort above that seen with measures of RV function alone.

4.6. Does RVFWS add significantly to the detection of this problem?

The recently published data by Li et al. [11], demonstrated a degree of longitudinal dysfunction in unselected patients hospitalised with COVID-19. Our subgroup analysis was slightly different; RVFWS demonstrated that RVFWS was not as sensitive as either RVFAC or RV VTI in identifying RV dysfunction. Therefore, we did not demonstrate significant additional benefit of RV strain imaging in critically ill COVID-19 patients. This is important, as many centres grapple with logistics in the current pandemic, it is key to be able to detect dysfunction within the capabilities of most critical care facilities using more widely available techniques.

4.7. Limitations

Firstly, the fact that the cohort studied were all critically ill in a tertiary centre with a number of patients on VV ECMO suggests the findings of this study may not be generalizable to other cohorts. All patients in this cohort had confirmed COVID-19. No control data was available from a non-COVID cohort, therefore, it is not possible to compare our findings directly with other groups of patients with ARDS. Secondly, the provision of a comprehensive quantitative echocardiographic assessment may not be widely available. Thirdly, our sample size, despite being comparatively larger than many previous ARDS studies, is still relatively small and subject to the inherent limitations of smaller cohorts. Finally, the associations that we have demonstrated require validation in similar cohorts.

5. Conclusion

Severe COVID-19 ARDS is associated with a specific phenotype of RV dysfunction that has not previously been reported in this cohort. Spared longitudinal function means RV FAC, rather than TAPSE, could be considered as the measurement of choice in defining RV function in critically ill patients with COVID-19. The measurement of RV-PA coupling seems to provide additional information on the causes and consequences of RV impairment in this condition. The specific phenotype of radial dysfunction identified here should alert clinicians of the need to avoid interpretation of RV health purely on long-axis parameters.

Disclosures

None.

References

[1] J. Parr, Pneumonia in China: lack of information raises concerns among Hong Kong health workers, BMJ. 368 (2020) m56.

[2] Organisation WH, https://www.who.int/emergencies/diseases/novel-coronavirus-2019.

[3] Z. Wu, J.M. McGoogan, Characteristics of and important lessons from the coronavirus disease 2019 (COVID-19) outbreak in China: summary of a report of 72314 cases from the Chinese Center for Disease Control and Prevention, JAMA (2020) 1239–1242.

[4] S. Shi, M. Qin, B. Shen, Y. Cai, T. Liu, F. Yang, et al., Association of cardiac injury with mortality in hospitalized patients with COVID-19 in Wuhan, China, JAMA Cardiol. (2020) 802–810.

[5] T. Guo, Y. Fan, M. Chen, X. Wu, L. Zhang, T. He, et al., Cardiovascular implications of fatal outcomes of patients with coronavirus disease 2019 (COVID-19), JAMA Cardiol. (2020) 1–8.

[6] S. Bangalore, A. Sharma, A. Slotwiner, L. Yatskar, R. Harari, B. Shah, et al., ST-segment elevation in patients with covid-19 - a case series, N. Engl. J. Med. (2020) 2470–2478.

[7] Cardiology ESo, ESC Guidance for the Diagnosis and Management of CV Disease During the COVID-19 Pandemic, 2020.

[8] J.N. Kirkpatrick, C. Mitchell, C. Taub, S. Kort, J. Hung, M. Swaminathan, ASE statement on protection of patients and echocardiography service providers during the 2019 novel coronavirus outbreak, J. Am. Coll. Cardiol. (2020) 648–653.

[9] B. Evrard, M. Goudelin, N. Montmagnon, A.L. Fedou, T. Lafon, P. Vignon, Cardiovascular phenotypes in ventilated patients with COVID-19 acute respiratory distress syndrome, Crit. Care 24 (1) (2020) 236.

[10] Q. Deng, B. Hu, Y. Zhang, H. Wang, X. Zhou, W. Hu, et al., Suspected myocardial injury in patients with COVID-19: evidence from front-line clinical observation in Wuhan, China, Int. J. Cardiol. (2020) 116–121.

[11] H.L. Yuman Li, Shuangshuang Zhu, Yuji Xie, Bin Wang, Lin He, Danqing Zhang, Yongxing Zhang, Hongliang Yuan, Chun Wu, Wei Sun, Yanting Zhang, Meng Li, Li Cui, Yu Cai, Jing Wang, Yali Yang, Qing Lv, Li Zhang, Mingxing Xie, Prognostic Value od Right Ventricular Longitudinal Strain in Patients with COVID-19, JACC Cardiovasc. Imaging (2020) 2287–2299.

[12] J.F. Murray, M.A. Matthay, J.M. Luce, M.R. Flick, An expanded definition of the adult respiratory distress syndrome, Am. Rev. Respir. Dis. 138 (3) (1988) 720–723.

[13] R.M. Lang, L.P. Badano, V. Mor-Avi, J. Afilalo, A. Armstrong, L. Ernande, et al., Recommendations for cardiac chamber quantification by echocardiography in adults: an update from the American Society of Echocardiography and the European Association of Cardiovascular Imaging, J. Am. Soc. Echocardiogr. 28 (1) (2015) 1-39.e14.

[14] A.R. Opotowsky, M. Clair, J. Afilalo, M.J. Landzberg, A.B. Waxman, L. Moko, et al., A simple echocardiographic method to estimate pulmonary vascular resistance, Am. J. Cardiol. 112 (6) (2013) 873–882.

[15] S.F. Nagueh, O.A. Smiseth, C.P. Appleton, B.F. Byrd, H. Dokainish, T. Edvardsen, et al., Recommendations for the evaluation of left ventricular diastolic function by echocardiography: an update from the American Society of Echocardiography and the European Association of Cardiovascular Imaging, Eur. Heart J. Cardiovasc. Imaging 17 (12) (2016) 1321–1360.

[16] Y. Topilsky, J.K. Oh, D.K. Shah, B.A. Boilson, J.A. Schirger, S.S. Kushwaha, et al., Echocardiographic predictors of adverse outcomes after continuous left ventricular assist device implantation, JACC Cardiovasc. Imaging 4 (3) (2011) 211–222.

[17] M. Guazzi, D. Dixon, V. Labate, L. Beussink-Nelson, F. Bandera, M.J. Cuttica, et al., RV contractile function and its coupling to pulmonary circulation in heart failure with preserved ejection fraction: stratification of clinical phenotypes and outcomes, JACC Cardiovasc. Imaging 10 (10 Pt B) (2017) 1211–1221.

[18] S.K. Wadia, T.G. Shah, G. Hedstrom, J.A. Kovach, R. Tandon, Early detection of right ventricular dysfunction using transthoracic echocardiography in ARDS: a more objective approach, Echocardiography. 33 (12) (2016) 1874–1879.

[19] T.G. Shah, S.K. Wadia, J. Kovach, L. Fogg, R. Tandon, Echocardiographic parameters of right ventricular function predict mortality in acute respiratory distress syndrome: a pilot study, Pulm. Circ. 6 (2) (2016) 155–160.

[20] D. Osman, X. Monnet, V. Castelain, N. Anguel, J. Warszawski, J.L. Teboul, et al., Incidence and prognostic value of right ventricular failure in acute respiratory distress syndrome, Intensive Care Med. 35 (1) (2009) 69–76.

[21] C. Creel-Bulos, M. Hockstein, N. Amin, S. Melhem, A. Truong, M. Sharifpour, Acute Cor pulmonale in critically ill patients with Covid-19, N. Engl. J. Med. 382 (21) (2020), e70, .

[22] M. Pagnesi, L. Baldetti, A. Beneduce, F. Calvo, M. Gramegna, V. Pazzanese, et al., Pulmonary hypertension and right ventricular involvement in hospitalised patients with COVID-19, Heart. 106 (17) (2020) 1324–1331.

[23] A. D'Andrea, R. Scarafile, L. Riegler, B. Liccardo, F. Crescibene, R. Cocchia, et al., Right ventricular function and pulmonary pressures as independent predictors of survival in patients with COVID-19 pneumonia, JACC Cardiovasc. Imaging (2020) 2467–2468.

[24] V. Zochios, K. Parhar, W. Tunnicliffe, A. Roscoe, F. Gao, The right ventricle in ARDS, Chest. 152 (1) (2017) 181–193.

[25] M.R. Dweck, A. Bularga, R.T. Hahn, R. Bing, K.K. Lee, A.R. Chapman, et al., Global evaluation of echocardiography in patients with COVID-19, Eur. Heart J. Cardiovasc. Imaging 21 (9) (2020) 949–958.

[26] Y. Li, H. Li, S. Zhu, Y. Xie, B. Wang, L. He, et al., Prognostic value of right ventricular longitudinal strain in patients with COVID-19, JACC Cardiovasc. Imaging (2020) 2287–2299.

[27] M. Focardi, M. Cameli, S.F. Carbone, A. Massoni, R. De Vito, M. Lisi, et al., Traditional and innovative echocardiographic parameters for the analysis of right ventricular performance in comparison with cardiac magnetic resonance, Eur. Heart J. Cardiovasc. Imaging 16 (1) (2015) 47–52.

[28] E. Argulian, K. Sud, B. Vogel, C. Bohra, V.P. Garg, S. Talebi, et al., Right ventricular dilation in hospitalized patients with COVID-19 infection, JACC Cardiovasc. Imaging (2020) 2459–2461.

[29] K.W. Scheel, S.E. Williams, J.B. Parker, Coronary sinus pressure has a direct effect on gradient for coronary perfusion, Am. J. Phys. 258 (6 Pt 2) (1990) H1739–H1744.

[30] R.P. Kelly, C.T. Ting, T.M. Yang, C.P. Liu, W.L. Maughan, M.S. Chang, et al., Effective arterial elastance as index of arterial vascular load in humans, Circulation. 86 (2) (1992) 513–521.

[31] W.J. Sibbald, A.A. Driedger, Right ventricular function in acute disease states: pathophysiologic considerations, Crit. Care Med. 11 (5) (1983) 339–345.

[32] V. Zochios, N. Jones, Acute right heart syndrome in the critically ill patient, Heart Lung Vessel 6 (3) (2014) 157–170.

[33] L.P. Badano, C. Ginghina, J. Easaw, D. Muraru, M.T. Grillo, P. Lancellotti, et al., Right ventricle in pulmonary arterial hypertension: haemodynamics, structural changes, imaging, and proposal of a study protocol aimed to assess remodelling and treatment effects, Eur. J. Echocardiogr. 11 (1) (2010) 27–37.

[34] A.J. Swift, S. Rajaram, D. Capener, C. Elliot, R. Condliffe, J.M. Wild, et al., Longitudinal and transverse right ventricular function in pulmonary hypertension: cardiovascular magnetic resonance imaging study from the ASPIRE registry, Pulm. Circ. 5 (3) (2015) 557–564.

[35] A. Kovács, B. Lakatos, M. Tokodi, B. Merkely, Right ventricular mechanical pattern in health and disease: beyond longitudinal shortening, Heart Fail. Rev. 24 (4) (2019) 511–520.

[36] V.P. Harjola, A. Mebazaa, J. Čelutkienė, D. Bettex, H. Bueno, O. Chioncel, et al., Contemporary management of acute right ventricular failure: a statement from the heart failure association and the working group on pulmonary circulation and right ventricular function of the European Society of Cardiology, Eur. J. Heart Fail. 18 (3) (2016) 226–241.

[37] A. Paternot, X. Repesse, A. Vieillard-Baron, Rationale and description of right ventricle-protective ventilation in ARDS, Respir. Care 61 (10) (2016) 1391–1396.

[38] A. Vieillard-Baron, Y. Loubieres, J.M. Schmitt, B. Page, O. Dubourg, F. Jardin, Cyclic changes in right ventricular output impedance during mechanical ventilation, J. Appl. Physiol. 87 (5) (1999) 1644–1650.

[39] J.M. Schmitt, A. Vieillard-Baron, R. Augarde, S. Prin, B. Page, F. Jardin, Positive end-expiratory pressure titration in acute respiratory distress syndrome patients: impact on right ventricular outflow impedance evaluated by pulmonary artery Doppler flow velocity measurements, Crit. Care Med. 29 (6) (2001) 1154–1158.

[40] M. Ackermann, S.E. Verleden, M. Kuehnel, A. Haverich, T. Welte, F. Laenger, et al., Pulmonary vascular Endothelialitis, thrombosis, and angiogenesis in Covid-19, N. Engl. J. Med. (2020) 120–128.

[41] J. Helms, C. Tacquard, F. Severac, I. Leonard-Lorant, M. Ohana, X. Delabranche, et al., High risk of thrombosis in patients with severe SARS-CoV-2 infection: a multicenter prospective cohort study, Intensive Care Med. (2020) 1–10.

[42] J.I. Weitz, J.C. Fredenburgh, J.W. Eikelboom, A test in context: D-dimer, J. Am. Coll. Cardiol. 70 (19) (2017) 2411–2420.

[43] K. Knai, N.K. Skjaervold, A pig model of acute right ventricular afterload increase by hypoxic pulmonary vasoconstriction, BMC Res. Notes 10 (1) (2017) 2.